ACS APPLIED MATERIALS & INTERFACES

Research Article

www.acsami.org

Perovskite Solar Cell with an Efficient TiO_2 Compact Film

Weijun Ke,[†,‡] Guojia Fang,[*,†,‡] Jing Wang,[†] Pingli Qin,[†] Hong Tao,[†] Hongwei Lei,[†] Qin Liu,[†] Xin Dai,[†] and Xingzhong Zhao[†]

[†]Key Laboratory of Artificial Micro- and Nano-Structures of the Ministry of Education of China, Department of Electronic Science and Technology, School of Physics and Technology, Wuhan University, Wuhan 430072, People's Republic of China

[‡]Shenzhen Institute, Wuhan University, Shenzhen 518055, People's Republic of China

ABSTRACT: A perovskite solar cell with a thin TiO_2 compact film prepared by thermal oxidation of sputtered Ti film achieved a high efficiency of 15.07%. The thin TiO_2 film prepared by thermal oxidation is very dense and inhibits the recombination process at the interface. The optimum thickness of the TiO_2 compact film prepared by thermal oxidation is thinner than that prepared by spin-coating method. Also, the TiO_2 compact film and the TiO_2 porous film can be sintered at the same time. This one-step sintering process leads to a lower dark current density, a lower series resistance, and a higher recombination resistance than those of two-step sintering. Therefore, the perovskite solar cell with the TiO_2 compact film prepared by thermal oxidation has a higher short-circuit current density and a higher fill factor.

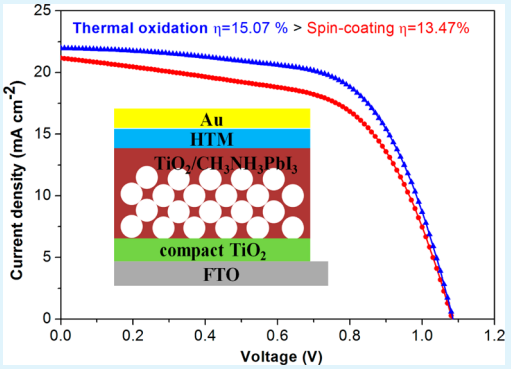

KEYWORDS: *perovskite, solar cell, compact electron transporting layer, interface resistance, one-step sintering*

1. INTRODUCTION

Perovskites with the general formula ABX_3 have octahedral and cuboctahedral geometries, where A and B cations coordinate with 6 and 12 X anions, respectively.[1−3] Recently, as a new class of light-harvesting materials for solar cells, organo-lead halide perovskites have attracted extensive attention due to their solution processability,[4] high charge carrier mobilities,[1] tunable optical properties,[5] and large absorption coefficient.[6] Organo-metal halide perovskites as sensitizers in liquid electrolyte-based dye-sensitized solar cells (DSSCs) have achieved a power conversion efficiency (PCE) of 3.8%.[7] An all-solid-state lead iodide perovskite sensitized TiO_2 mesoscopic heterojunction solar cell has showed a PCE of 9.7%, which has long-term stability.[8] A very high PCE of 15.0% has been obtained for perovskite-sensitized mesoscopic solar cells prepared by a sequential deposition method.[9]

Many researches have been focused on DSSC since Grätzel reported a low-cost and high-efficiency DSSC with a sandwich-type structure in 1991.[10] The conventional DSSC has a dye-sensitized photoanode, a counter electrode, and an electrolyte.[11] The photoanode includes a TiO_2 porous film and a TiO_2 compact film.[12] The TiO_2 compact film is usually sintered at a high temperature, followed by a TiO_2 porous film. Therefore, the films are sintered twice at a high temperature. The thickness of the TiO_2 porous film is more than 10 μm. The TiO_2 porous layer composed of 20 nm particles is deposited by a doctor-blade method.[13] The TiO_2 compact layer is traditionally prepared by aerosol spray pyrolysis,[14−16] thermal oxidation,[17] spin-coating method,[12] atomic layer deposition,[18] and electrochemical deposition.[19] A few tens of nanometers TiO_2 compact film is included, which inhibits the recombination and avoids electrolyte direct contact with the conductive substrate.[15] The above-mentioned perovskite solar cells also include a TiO_2 porous film and a TiO_2 compact film. However, for the perovskite solar cells, a few hundreds of nanometers of the TiO_2 porous film is enough to absorb the perovskite.[8] A solar cell with a thin TiO_2 porous film shows a high short-circuit current density (J_{sc}), open-circuit voltage (V_{oc}), and fill factor (FF).[8] The absorption coefficient of perovskite is estimated to be 10 times higher than that of the conventional N719 dye.[6] The perovskite $CH_3NH_3PbI_3$ has long electron and hole transporting lengths.[20] On one hand, the thickness of the TiO_2 porous film is critical to the perovskite solar cells.[21] The thickness of the peroskite film is usually determined by the TiO_2 porous film. In order to form an anatase, the TiO_2 porous film must be sintered at a high temperature. On the other hand, the compact film also greatly impacts the performance of the perovskite solar cells. Recently, Snaith et al. reported that the perovskite solar cells with a thin electron transporting layer of graphene/TiO_2 nanocomposites achieved a very high efficiency (15.6%).[22] DSSCs with various compact films prepared by different methods have been reported; however, little research on the compact films for the perovskite solar cells has been carried out. Han et al. reported the TiO_2 compact film prepared by atomic layer deposition, spin-coating, and spray pyrolysis methods.[23] However, TiO_2 compact film prepared by thermal oxidation method (TO-TiO_2 compact film) has not been reported. An efficient TiO_2 compact film prepared by a simple

Received: June 12, 2014
Accepted: August 28, 2014
Published: August 28, 2014

method is very important to achieve a low cost and high PCE for the perovskite solar cells.

In this study, we report a novel method to prepare the TiO_2 compact layer and the TiO_2 porous layer for the perovskite solar cells. A thin Ti film was sputtered from a Ti target and a thin layer of porous TiO_2 paste was spin coated on it before it was thermally annealed at 500 °C for 30 min. Therefore, the TiO_2 porous film and the TiO_2 compact film were obtained by this one-step sintering process at one time. To the best of our knowledge, it is the first time to report a one-step sintering method to prepare the TiO_2 porous film and the TiO_2 compact film for the perovskite solar cell applications. It can not only reduce the cost, but also improve the PCE of the device. A low series resistance, a high recombination resistance, and a low charge transfer resistance have been received due to the formation of the TiO_2 compact layer with the porous TiO_2 at the same time. The perovskite solar cell with the TiO_2 compact film prepared by thermal oxidation has achieved a higher PCE than that with the TiO_2 compact film prepared by spin-coating method (SC-TiO_2 compact film).

2. EXPERIMENTAL DETAILS

2.1. Materials. 2,2′,7,7′-tetrakis(*N*,*N*-di-*p*-methoxyphenylamine)-9,9′-spirobifluorene (spiro-OMeTAD) (≥99.0%) was purchased from Shenzhen Feiming Science and Technology Co., Ltd. Li-bis-(trifluoromethanesulfonyl) imide (Li-TFSI), 4-*tert*-butylpyridine (TBP) and lead iodide (PbI2) (99.9%) were purchased from Aladdin Reagents. Hydroiodic acid (57 wt % in water, 99.99%) and methylamine (33 wt % in absolute ethanol) were purchased from Sigma-Aldrich. Tetrabutyl titanate, ethanol, dimethylformamide, diethanolamine, and isopropanol were purchased from Sinopharm Chemical Reagent Co., Ltd. (China). All of the used reagents were analytical grade, without further purification. The purity of the gold used for thermal evaporation was 99.99%. Fluorine-doped tin oxide (FTO) glass was purchased from Asahi Glass (Japan) and had a sheet resistance of 14 Ω sq^{-1}.

2.2. Solar Cell Fabrication. The devices were fabricated on clean FTO glass substrates. A thin TiO_2 compact film was coated on FTO glass. The SC-TiO_2 compact film was prepared according to a standard procedure which has been reported in our previous work.[12,24] To prepare the precursor solution, 0.38 mL of diethanolamine, 1.8 mL of tetrabutyl titanate, and 18 mL of ethanol were stirred at 40 °C for 2 h. To form a sol, the solution should be aged for 24 h. A compact TiO_2 film was coated by spin-coating method with a low speed of 500 rpm for 6 s and at a high speed for 30 s. The thickness of the TiO_2 compact film was controlled by the high speed of the spin coater. After spin-coating, the film was thermally annealed at 500 °C for 30 min. Subsequently, a 400 nm TiO_2 porous film composed of 20 nm particles was coated on the compact film by spin-coating method and was heated at 500 °C for another 30 min. The SC-TiO_2 compact film and the TiO_2 porous film were prepared by a two-step sintering process. The TO-TiO_2 compact film was prepared by thermal oxidation of Ti film. Ti films with different thicknesses were coated on FTO glasses by radio frequency (RF) magnetron sputtering from a Ti target (99.9% purity). The RF power and sputtering pressure were 100 W and 1 Pa, respectively. The thickness of the Ti film was controlled by the time of sputtering. Subsequently, a 400 nm TiO_2 porous film composed of 20 nm particles was spin coated on the Ti film and was retained at 500 °C for 30 min. At the same time, the Ti film was oxidized to a TiO_2 compact film. After thermal oxidation, the metallic Ti film became a transparent film. It is obvious that the Ti film was completely oxidized and converted to a thin TiO_2 compact film. Therefore, the TO-TiO_2 compact film and the TiO_2 porous film were prepared by a one-step sintering process.

The perovskite $CH_3NH_3PbI_3$ was synthesized as reported in literature.[9,25] First, 39.3 mL of methylamine and 39.6 mL of hydroiodic acid at a 1:1 equimolar ratio were stirred at 0 °C for 2 h. The precipitate was collected by evaporating at 50 °C for 2 h. Finally, a white power was obtained by washing with diethyl ether three times and drying at 100 °C in a vacuum oven for 24 h. 1 mol/L PbI_2 (dissolved in dimethylformamide at 70 °C for 12 h) was spin coated onto the TiO_2 porous film at a speed of 2000 rpm for 45 s and was heated at 70 °C in the air for 30 min. Subsequently, the film was dipped into a solution of CH_3NH_3I (10 mg/mL, dissolved in isopropanol) for 2 min. Finally, the film was annealed at 70 °C in the air for 30 min. The hole transporting material (HTM) solution, consisting of 55 mM TBP, 26 mM Li-TFSI, and 68 mM spiro-OMeTAD dissolved in acetonitrile and chlorobenzene (1:10, v/v), was stirred at room temperature for 24 h and then was coated on the perovskite-sensitized TiO_2 film by spin-coating method at a speed of 2000 rpm for 30 s. Finally, to complete the device, a thin gold electrode was deposited by thermal evaporation.

2.3. Characteristics. Film crystal structure of $CH_3NH_3PbI_3$ film was examined by X-ray diffraction (XRD, Bruker AXS, D8 Advance) with Cu Kα radiation under operation conditions of 40 kV and 40 mA. The morphologies of perovskite solar cells were observed by a high-resolution field emission scanning electron microscope (SEM, JSM 6700F). The thicknesses of the TO-TiO_2 compact films and the SC-TiO_2 compact films were measured by SEM. Incident photon-to-current conversion efficiency (IPCE) spectra were measured by a Model QE/IPCE system (PV Measurements, Inc.) in the 320−800 nm wavelength range. The square average roughnesses of the TiO_2 compact films were characterized by atomic force microscopy (AFM, SPM-9500j3). Transmission and absorption spectra were measured by an ultraviolet−visible (UV−vis) spectrophotometer (CARY 5000, Varian, Australia) at room temperature. The perovskite solar cells were irradiated by a standard ABET Sun 2000 Solar Simulator with a power density of 100 mW cm^{-2} (AM1.5 simulated irradiation). The active area of the perovskite solar cells was 0.09 cm^2. Photocurrent density−voltage (J−V) characteristics were performed on a CHI660D electrochemical workstation (ShangHai, China) with a scan rate of 100 mV s^{-1}. Electrochemical impedance spectroscopy (EIS) was performed on a CHI660D electrochemical workstation (ShangHai, China) with a 10 mV AC amplitude, a frequency ranging from 100 kHz to 0.1 Hz, and a 0.6 V bias under 1 sun illumination. Photoluminescence (PL) spectrum was obtained with a 532 nm pulsed laser as excitation source at a frequency of 9.743 MHz.

3. RESULTS AND DISCUSSION

In Figure 1, panels a and b show the device structure and energy level diagram of the perovskite solar cells, respectively.

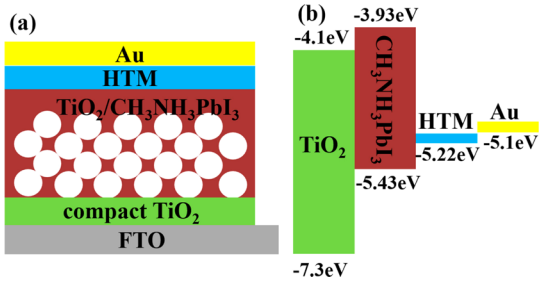

Figure 1. (a) Device structure and (b) energy level diagram of the perovskite solar cell.

The inorganic−organic hybrid heterojunction solar cells include a conductive substrate, a compact layer, a perovskite-sensitized TiO_2 porous layer, a hole transporting layer, and a metal electrode. The TiO_2 compact film transports the electron and inhibits recombination. Most light will be absorbed by the perovskite film. The matching band structure leads the electron and the hole to separate effectively. To achieve a high efficiency, a TiO_2 porous film with a compatible pore size and thickness should be filled with the perovskite film. Furthermore, to avoid

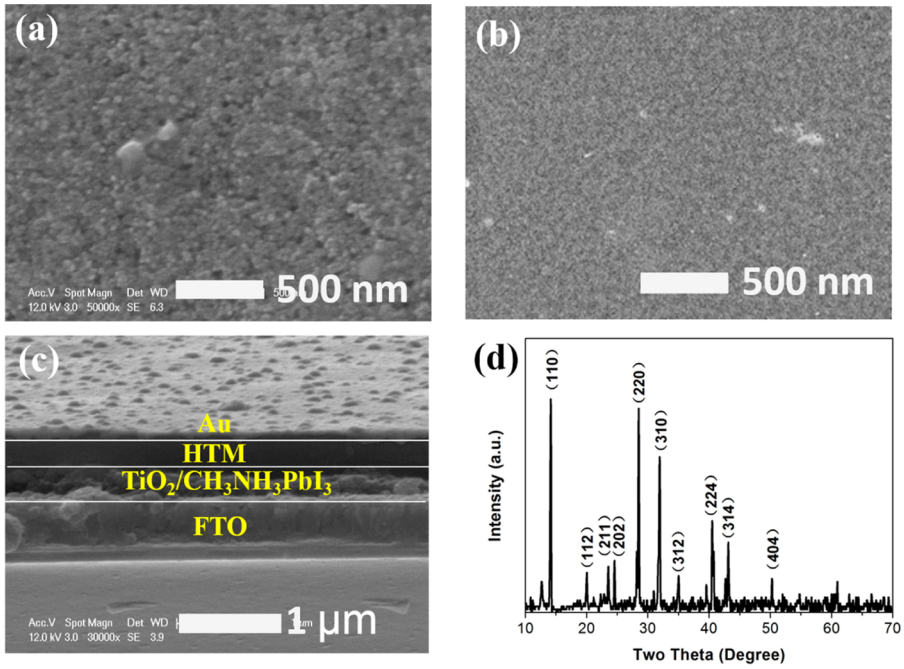

Figure 2. Top-view SEM images of (a) the perovskite $CH_3NH_3PbI_3$ on the TiO_2 porous film and (b) the HTM on the perovskite film. (c) Cross-sectional SEM image of the device. (d) XRD pattern of the perovskite $CH_3NH_3PbI_3$ film on the TiO_2 porous film.

contact with Au electrode directly, the perovskite-sensitized TiO_2 porous layer was covered with a thin hole transporting layer. Most importantly, the hole transporting layer favors the hole injecting to the Au electrode and blocking the electron transfer from the perovskite film to the Au electrode, which will led to a high FF and V_{oc}. Figure 2a shows a top-view SEM image of the perovskite $CH_3NH_3PbI_3$ on the TiO_2 porous film. The TiO_2 porous film with a few tens of nanometers of the pore size is filled with perovskite. Figure 2b shows a top-view SEM image of the HTM on the perovskite film. The smooth surface means that the perovskite is uniformly capped by the HTM. The cross-sectional SEM image of the device is shown in Figure 2c. The substrate is the FTO glass. As a light absorber, a 400 nm TiO_2 porous film is filled with the perovskite on the FTO. A 400 nm capping layer on the perovskite film is the HTM. The thin top layer is the Au electrode. To check the phase structure of $CH_3NH_3PbI_3$, a $CH_3NH_3PbI_3$ film was spin coated on a TiO_2 porous film. As shown in Figure 2d, the (110), (220), and (310) planes are included. The strong diffraction peaks of the film can be well indexed to a perovskite structure.[26−28] The UV−vis absorption spectrum of the perovskikte $CH_3NH_3PbI_3$ on the TiO_2 porous film shows an absorption peak at 760 nm (Figure 3a). The PL spectrum of the perovskite $CH_3NH_3PbI_3$ shows an emission peak at 760 nm, too (Figure 3b).

Figure 4a shows the $J-V$ curves of the perovskite solar cells with the SC-TiO_2 compact films. If a too thin SC-TiO_2 compact film was applied, the FTO will be not fully covered with the dense TiO_2 blocking layer, and the perovskite film will contact with FTO directly. Moreover, the serious recombination process will occur in the surface of the FTO, and the leakage current will be very large. If the interface is passivized, the interfacial recombination process will be controlled.[29] If a too thick SC-TiO_2 compact film is applied, the distance will be too large to transfer electron from the perovskite film to the FTO. Furthermore, a thicker TiO_2 compact film will result in weaker light absorption of the perovskite film. Therefore, with

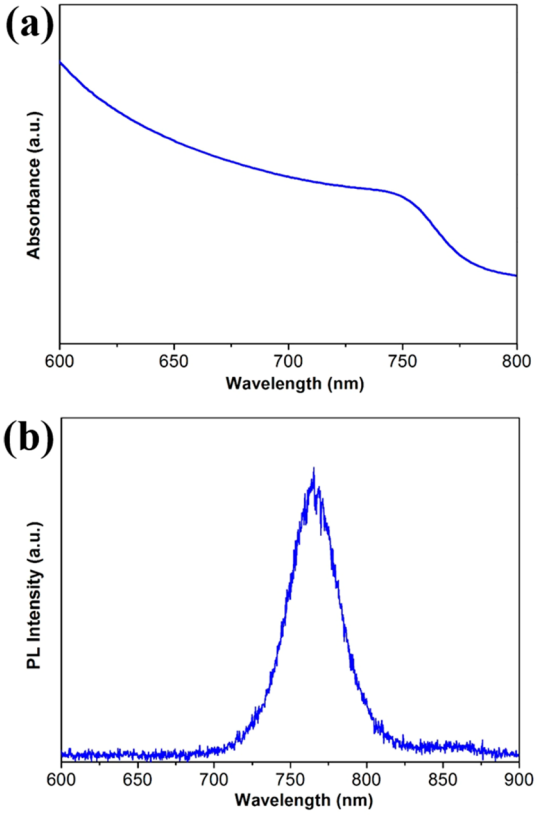

Figure 3. (a) UV−vis absorption and (b) PL spectra of perovskite $CH_3NH_3PbI_3$ on the TiO_2 porous film.

increasing thickness of the TiO_2 compact film, the performance of perovskite solar cells first increased and then decreased. The optimum thickness of the SC-TiO_2 compact film is about 60 nm, and a high PCE of 13.47% was obtained. Figure 4b shows the $J-V$ curves of the perovskite solar cells with the TO-TiO_2

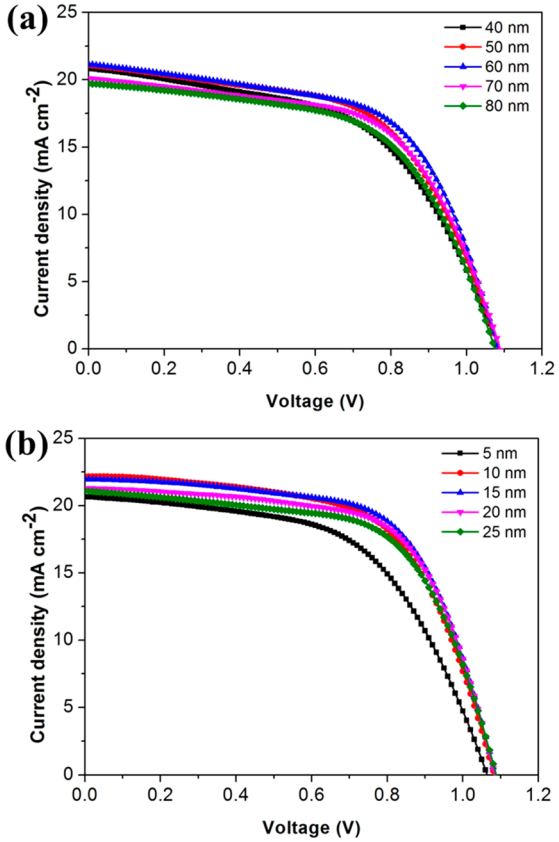

Figure 4. $J-V$ curves of the perovskite solar cells with different thicknesses of (a) SC-TiO_2 and (b) TO-TiO_2 compact films.

compact films. It is obvious that the optimum thickness of the TO-TiO_2 compact film is about 15 nm and a high PCE of 15.07% was obtained. The results are presented in Table 1. As

Table 1. Photovoltaic Parameters of the Perovskite Solar Cells

	V_{oc} (V)	J_{sc} (mA cm^{-2})	FF	PCE (%)	R_s (Ω cm^2)
bare	0.96	18.01	0.44	7.60	6.29
40 nm SC-TiO_2	1.09	20.83	0.53	12.04	5.49
50 nm SC-TiO_2	1.09	21.08	0.56	12.97	4.86
60 nm SC-TiO_2	1.09	21.16	0.58	13.47	3.97
70 nm SC-TiO_2	1.09	20.11	0.58	12.80	4.29
80 nm SC-TiO_2	1.08	19.72	0.57	12.20	4.67
5 nm TO-TiO_2	1.07	20.66	0.56	12.29	5.17
10 nm TO-TiO_2	1.09	22.19	0.60	14.59	4.32
15 nm TO-TiO_2	1.09	21.97	0.63	15.07	3.57
20 nm TO-TiO_2	1.09	21.30	0.64	14.76	3.76
25 nm TO-TiO_2	1.09	21.10	0.62	14.15	4.08

shown in Figure 5, the perovskite solar cell with the TO-TiO_2 compact film has received a higher PCE than that with the SC-TiO_2 compact film. The optimum thickness of the TiO_2 compact film is different for the two methods. If the compact film is absent, the performance of perovskite solar cells will be poor. To enhance the photoenergy conversion efficiency, it is necessary to block the dark current.[30] A compact layer between the FTO and the TiO_2 nanocrystals could increase the performance of solar cells.[30] It shows that the dark current density of the perovskite solar cell with the SC-TiO_2 compact

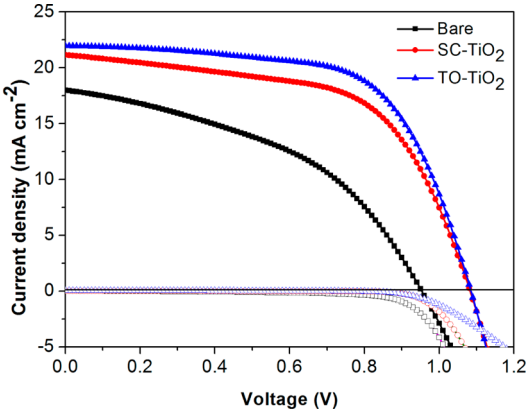

Figure 5. $J-V$ curves of the perovskite solar cells with the 15 nm TO-TiO_2 compact film, the 60 nm SC-TiO_2 compact film, and the bare FTO.

film is higher than that with the TO-TiO_2 compact film (Figure 5a). The compact film prepared by spin-coating method may has pinholes.[15,23] A thicker compact film prepared by spin-coating method is needed to cover the FTO. Therefore, the electron runs a longer distance. However, the FTO could be covered with a thin Ti film prepared by sputtering method, and a dense TiO_2 film was formed by thermal oxidation. A thinner and denser TiO_2 film was enough to cover the FTO. Moreover, the TO-TiO_2 compact film was sintered with the TiO_2 porous film at the same time. The interface resistance between the compact film and the porous film may be lower. It not only reduces production cost, but also reduces the interface recombination. Therefore, the perovskite solar cell with the TO-TiO_2 compact film has a lower dark current density than that with the SC-TiO_2 compact film. The dark current density of the perovskite solar cell without compact film is the highest. The recombination is serious for the perovskite solar cell without TiO_2 compact film, which is used as a hole blocking layer and an electron transporting layer. A shunting process is employed, and therefore, the perovskite solar cell without compact film has a lower J_{sc}, V_{oc}, and FF.

The series resistance (R_s) and shunt resistance (R_{sh}) can be calculated by the diode equation.[31] Figure 6a shows good linear curves, which indicate the relationship of -dV/dJ and $(J_{sc} - J)^{-1}$. The R_s of the bare FTO (without compact film but with porous film), the SC-TiO_2 compact film, and the TO-TiO_2 compact film are 6.29, 3.97, and 3.57 Ω cm^2, respectively. The R_{sh} of the bare FTO, the SC-TiO_2 compact film, and the TO-TiO_2 compact film are 180, 303, and 1800 Ω cm^2, respectively. The device without compact film has the highest R_s and the lowest R_{sh}. As the thickness of the TiO_2 blocking layer increased, the R_s decreased first and then increased. The results are summarized in Table 1. The device with a too thin blocking film, which is not fully covered with FTO, will have a serious recombination. Moreover, the TiO_2 compact film has a low electrical conductivity. Therefore, the device with a too thin blocking film or a too thick blocking film has a higher R_s. The device with the 15 nm TO-TiO_2 compact film has the lowest R_s and the highest R_{sh}. The low R_s and the high R_{sh} may lead to a high FF. These perovskite solar cells were fabricated in the same conditions, except the compact film. The different interface resistance may be one reason for the different photovoltaic properties. The TO-TiO_2 compact film was prepared by a one-step sintering method, and so, the optimum

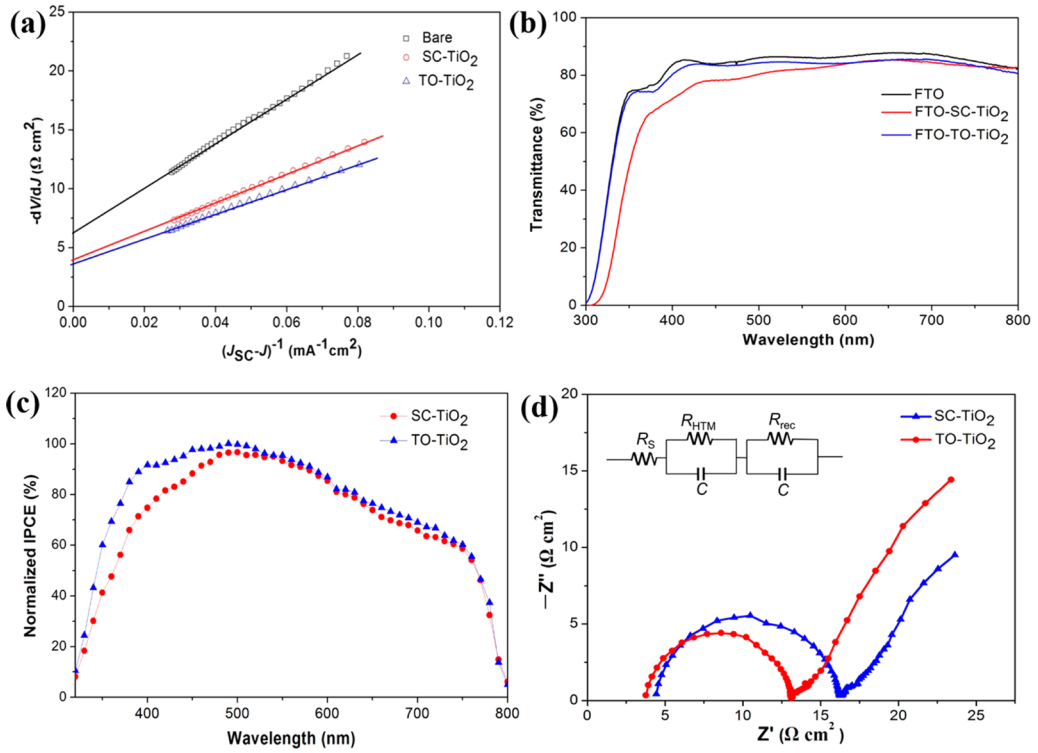

Figure 6. (a) The linear curves of the relationship of -dV/dJ and $(J_{sc} - J)^{-1}$. (b) Transmission spectra of the TO-TiO_2 compact film, the SC-TiO_2 compact film, and the bare FTO. (c) IPCE spectra and (d) Nyquist plot of the perovskite solar cells with the TO-TiO_2 compact film and the SC-TiO_2 compact film.

TO-TiO_2 compact film is thinner than that of the optimum SC-TiO_2 compact film. Therefore, the perovskite solar cell with the TO-TiO_2 compact film has a higher FF and J_{sc}. Figure 6b shows the transmission spectra of the TO-TiO_2 compact film on FTO, the SC-TiO_2 compact film on FTO, and the bare FTO. The thicknesses of the TO-TiO_2 compact film and the SC-TiO_2 compact film are about 15 and 60 nm, respectively. The optimum thickness of the SC-TiO_2 compact film is thicker than that of the TO-TiO_2 compact film. As we know, TiO_2 is a wide band gap semiconductor, which has a strong absorption at short wavelengths.[32,33] The thinner TO-TiO_2 compact film is more transparent than the SC-TiO_2 compact film between 300 and 550 nm. A 60 nm SC-TiO_2 compact film on FTO has a stronger absorption than a 15 nm TO-TiO_2 film at 300−550 nm. Therefore, more light will be absorbed by perovskite and will be converted to photocurrent for the perovskite solar cell by employing the TO-TiO_2 compact film. It may lead the perovskite solar cell with the TO-TiO_2 compact film to a higher J_{sc}. This result also corresponds to the normalized IPCE curves of the SC-TiO_2 compact film and the TO-TiO_2 compact film in Figure 6c. It shows that the perovskite solar cell with the TO-TiO_2 compact film has a higher IPCE values than that with the SC-TiO_2 compact film at a short wavelength range. Therefore, the perovskite solar cell with the TO-TiO_2 compact film has a higher J_{sc}. The perovskite solar cell has a high IPCE value in the 400−760 nm wavelength range. The IPCE intensity dropped at a wavelength longer than 760 nm. This result is similar to some literature reports.[8,9,31] It may be due to the perovskite $CH_3NH_3PbI_3$ film having a strong absorption in the visible spectrum (it has an absorption peak at 760 nm, Figure 3a); however, it has a weak absorption in the infrared wavelength range. To understand the charge transfer and recombination rates, Nyquist plots of the perovskite solar cells with the SC-TiO_2 compact film and the TO-TiO_2 compact film are shown in Figure 6d. The R_S is equal to the value of high-frequency intercept on the real axis. The right incomplete semicircle in the low frequency range is a transmission line, which is mainly attributed to recombination resistance (R_{rec}) between the perovskite film and the TiO_2 film.[34−37] The left semicircle in the high frequency range is assigned to the charge transfer resistance (R_{HTM}) at the hole transporting layer.[34−36] The R_S of the SC-TiO_2 compact film and the TO-TiO_2 compact film are 4.44 and 3.77 Ω cm^2, respectively. The values of the R_S for the EIS results correspond to the values calculated by the diode equation. It shows that the perovskite solar cell with the TO-TiO_2 compact film has a lower R_S and R_{HTM} than that with the SC-TiO_2 compact film. Therefore, the perovskite solar cell with the TO-TiO_2 compact film has a higher charge transfer rate. Moreover, the perovskite solar cell with the TO-TiO_2 compact film has a higher R_{rec} than that with the SC-TiO_2 compact film. The thinner TO-TiO_2 compact film prepared by one-step sintering method may lead to a lower interface resistance, a lower R_S, and a higher R_{rec} than those of the thicker SC-TiO_2 compact film prepared by the two-step sintering method. It also indicates that the perovskite solar cell with the TO-TiO_2 compact film has a lower carrier recombination rate. The perovskite solar cell has a large and wide absorption in the visible spectrum, which leads to a high IPCE value in a wide wavelength. Moreover, the device has a low series resistance, a high shunt resistance, a low charge transfer resistance, and a high recombination resistance. Therefore, the perovskite solar cell has a J_{sc}, V_{oc}, and FF. Above all, the perovskite $CH_3NH_3PbI_3$ has 100 nanometers of electron−hole diffusion lengths.[20] Time-resolved PL measurements demonstrated that the electron had a long lifetime.[20] Therefore, the perovskite $CH_3NH_3PbI_3$ has a high electron transport rate and a low

dx.doi.org/10.1021/am503728d | ACS Appl. Mater. Interfaces 2014, 6, 15959−15965

carrier recombination rate. We confirmed this with EIS measurements. Therefore, the perovskite solar cell with the TO-TiO_2 compact film has a maximum PCE of 15.07%.

In Figure 7, panels a and b show the AFM images of the SC-TiO_2 compact film (60 nm) and the TO-TiO_2 compact film

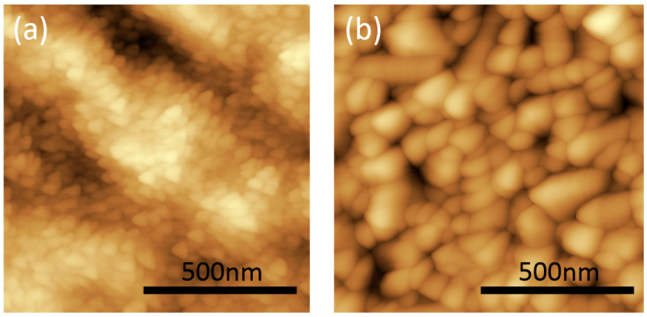

Figure 7. AFM images of (a) SC-TiO_2 and (b) TO-TiO_2 compact films on FTO.

(15 nm), respectively. The SC-TiO_2 compact film has a smoother surface than the TO-TiO_2 compact film. The square average roughnesses of the SC-TiO_2 compact film and the TO-TiO_2 compact film are 3.51 and 14.48 nm, respectively. However, the TO-TiO_2 compact film has a similar square average roughness with the bare FTO, which has a square average roughness of 15.16 nm. A very thin TO-TiO_2 compact film is enough to cover the FTO. Therefore, the square average roughness of the TO-TiO_2 compact film is also determined by the surface of FTO. A thicker SC-TiO_2 compact film is needed to cover the FTO. A smoother surface is received. However, it has a higher R_s and a lower R_{sh}. Above all, the TO-TiO_2 compact film and the TiO_2 porous film, which were prepared by a one-step sintering process, effectively reduced the cost and achieved a higher PCE (15.07%) than films prepared by a two-step sintering process. The Ti film could be prepared by a magnetron sputtering method, which has a fast sputtering rate by using a Ti target. It has an advantage of low-cost and large-area fabrication. If a TiO_2 target were applied, then a longer sputtering time will be needed. The crystallinity of the TiO_2 film prepared by a TiO_2 target without annealed is poor, which may lead to a low PCE. Moreover, when the sputtered Ti film and the TiO_2 porous film were sintered and crystallized at the same time, its interface effect will be reduced to minimum compared with using TiO_2 densified layer. The interface recombination has been reduced, which is rated to the interface resistance and R_s.

4. CONCLUSION

In summary, we have developed a perovskite solar cell with an efficient TiO_2 compact film. A very thin TiO_2 compact film and a TiO_2 porous film were prepared by a novel one-step sintering process. The TiO_2 compact film as a blocking layer inhibits the electron−hole recombination at the interface between the FTO and the perovskite. Furthermore, the one-step sintering method reduces the interface resistance between the TiO_2 compact film and the TiO_2 porous film and requres thinner densified TiO_2 layer. The lowest R_s (3.57 Ω cm^2) and the highest R_{sh} (1800 Ω cm^2) have been achieved by the device based on the TO-TiO_2 compact film. A maximum PCE of 15.07% has been achieved by the perovskite solar cell with the TO-TiO_2 compact film, which has a higher J_{sc} and FF than that with the SC-TiO_2 compact film. This method has a potential to be applied in high-efficiency, large-area, and low-cost perovskite solar cells in the future.

AUTHOR INFORMATION

Corresponding Author

*Tel: +86 (0)27 68752147. Fax: +86 (0)27 68752569. E-mail: gjfang@whu.edu.cn.

Notes

The authors declare no competing financial interest.

ACKNOWLEDGMENTS

This work was supported by the National Basic Research Program (No.2011CB933300) of China, Shenzhen Strategic Emerging Industry Development Funds (JCYJ20130401160028796), the Research Program of Wuhan Science and Technology Bureau (2013010501010141), the China Postdoctoral Science Foundation (2013M531737), and the Fundamental Research Funds for the Central Universities (2014202020207).

REFERENCES

(1) Kagan, C. R. Organic−Inorganic Hybrid Materials As Semiconducting Channels in Thin-Film Field-Effect Transistors. *Science* **1999**, *286*, 945−947.

(2) Mitzi, D. B.; Feild, C. A.; Harrison, W. T. A.; Guloy, A. M. Conducting Tin Halides with a Layered Organic-based Perovskite Structure. *Nature* **1994**, *369*, 467−469.

(3) Kim, H. S.; Im, S. H.; Park, N. G. Organolead Halide Perovskite: New Horizons in Solar Cell Research. *J. Phys. Chem. C* **2014**, *118*, 5615−5625.

(4) Kazim, S.; Nazeeruddin, M. K.; Grätzel, M.; Ahmad, S. Perovskite as Light Harvester: A Game Changer in Photovoltaics. *Angew. Chem., Int. Ed.* **2014**, *53*, 2812−2824.

(5) Kulkarni, S. A.; Baikie, T.; Boix, P. P.; Yantara, N.; Mathews, N.; Mhaisalkar, S. G. Band Gap Tuning of Lead Halide Perovskites Using a Sequential Deposition Process. *J. Mater. Chem. A* **2014**, *2*, 9221−9225.

(6) Im, J. H.; Lee, C. R.; Lee, J. W.; Park, S. W.; Park, N. G. 6.5% Efficient Perovskite Quantum-Dot-Sensitized Solar Cell. *Nanoscale* **2011**, *3*, 4088−4093.

(7) Kojima, A.; Teshima, K.; Shirai, Y.; Miyasaka, T. Organometal Halide Perovskites as Visible-Light Sensitizers for Photovoltaic Cells. *J. Am. Chem. Soc.* **2009**, *131*, 6050−6051.

(8) Kim, H. S.; Lee, C. R.; Im, J. H.; Lee, K. B.; Moehl, T.; Marchioro, A.; Moon, S. J.; Humphry-Baker, R.; Yum, J. H.; Moser, J. E.; Grätzel, M.; Park, N. G. Lead Iodide Perovskite Sensitized All-Solid-State Submicron Thin Film Mesoscopic Solar Cell with Efficiency Exceeding 9%. *Sci. Rep.* **2012**, *2*, 591.

(9) Burschka, J.; Pellet, N.; Moon, S. J.; Humphry-Baker, R.; Gao, P.; Nazeeruddin, M. K.; Grätzel, M. Sequential Deposition as a Route to High-Performance Perovskite-Sensitized Solar Cells. *Nature* **2013**, *499*, 316−319.

(10) O'Regan, B.; Grätzel, M. A Low-Cost, High-Efficiency Solar Cell Based on Dye-Sensitized Colloidal TiO_2 Films. *Nature* **1991**, *353*, 24.

(11) Grätzel, M. Dye-Sensitized Solar Cells. *J. Photochem. Photobiol., C* **2003**, *4*, 145−153.

(12) Ke, W. J.; Fang, G. J.; Lei, H. W.; Qin, P. L.; Tao, H.; Zeng, W.; Wang, J.; Zhao, X. Z. An Efficient and Transparent CuS Nanosheet Film Counter Electrode for Bifacial Quantum-Dot-Sensitized Solar Cells. *J. Power Sources* **2014**, *248*, 809−815.

(13) Zeng, W.; Fang, G. J.; Li, B. R.; Liu, Z. Q.; Han, T. Y.; Wang, J.; Liu, F. W.; Fang, P. F.; Zhao, X. Z.; Zou, D. C. Vibration Test Method to Study Elastic Stability of Porous Carbon Nanocomposite Counter Electrode in Dye Sensitized Solar Cells. *ACS Appl. Mater. Interfaces* **2013**, *5*, 7101−7108.

(14) Unger, E. L.; Spadavecchia, F.; Nonomura, K.; Palmgren, P.; Cappelletti, G.; Hagfeldt, A.; Johansson, E. M.; Boschloo, G. Effect of the Preparation Procedure on the Morphology of Thin TiO_2 Films and Their Device Performance in Small-Molecule Bilayer Hybrid Solar Cells. *ACS Appl. Mater. Interfaces* **2012**, *4*, 5997−6004.
(15) Kavan, L.; Tétreault, N.; Moehl, T.; Grätzel, M. Electrochemical Characterization of TiO_2 Blocking Layers for Dye-Sensitized Solar Cells. *J. Phys. Chem. C* **2014**, *118*, 16408−16418.
(16) Cameron, P. J.; Peter, L. M. Characterization of Titanium Dioxide Blocking Layers in Dye-Sensitized Nanocrystalline Solar Cells. *J. Phys. Chem. B* **2003**, *107*, 14394−14400.
(17) Xia, J. B.; Masaki, N.; Jiang, K. J.; Yanagida, S. Deposition of a Thin Film of TiO_x From a Titanium Metal Target as Novel Blocking Layers at Conducting Glass/TiO_2 Interfaces in Ionic Liquid Mesoscopic TiO_2 Dye-Sensitized Solar Cells. *J. Phys. Chem. B* **2006**, *110*, 25222−25228.
(18) Chandiran, A. K.; Yella, A.; Stefik, M.; Heiniger, L. P.; Comte, P.; Nazeeruddin, M. K.; Graätzel, M. Low-temperature Crystalline Titanium Dioxide by Atomic Layer Deposition for Dye-Sensitized Solar Cells. *ACS Appl. Mater. Interfaces* **2013**, *5*, 3487−3493.
(19) Kavan, L.; O'Regan, B.; Kay, A.; Grätzel, M. Preparation of TiO_2 (Anatase) Films on Electrodes by Anodic Oxidative Hydrolysis of $TiCl_3$. *J. Electroanal. Chem.* **1993**, *346*, 291−307.
(20) Xing, G. C.; Mathews, N.; Sun, S. Y.; Lim, S. S.; Lam, Y. M.; Grätzel, M.; Mhaisalkar, S.; Sum, T. C. Long-Range Balanced Electron- and Hole-Transport Lengths in Organic−Inorganic $CH_3NH_3PbI_3$. *Science* **2013**, *342*, 344−347.
(21) Heo, J. H.; Im, S. H.; Noh, J. H.; Mandal, T. N.; Lim, C. S.; Chang, J. A.; Lee, Y. H.; Kim, H. j.; Sarkar, A.; Nazeeruddin, M. K.; Grätzel, M.; Seok, S. I. Efficient Inorganic−Organic Hybrid Heterojunction Solar Cells Containing Perovskite Compound and Polymeric Hole Conductors. *Nat. Photonics* **2013**, *7*, 486−491.
(22) Wang, J. T.; Ball, J. M.; Barea, E. M.; Abate, A.; Alexander-Webber, J. A.; Huang, J.; Saliba, M.; Mora-Sero, I.; Bisquert, J.; Snaith, H. J.; Nicholas, R. J. Low-Temperature Processed Electron Collection Layers of Graphene/TiO_2 Nanocomposites in Thin Film Perovskite Solar Cells. *Nano Lett.* **2014**, *14*, 724−730.
(23) Wu, Y. Z.; Yang, X. D.; Chen, H.; Zhang, K.; Qin, C. J.; Liu, J.; Peng, W. Q.; Islam, A.; Bi, E. B.; Ye, F.; Yin, M. S.; Zhang, P.; Han, L. Y. Highly Compact TiO_2 Layer for Efficient Hole-Blocking in Perovskite Solar Cells. *Appl. Phys. Express* **2014**, *7*, 052301.
(24) Ke, W. J.; Fang, G. J.; Tao, H.; Qin, P. L.; Wang, J.; Lei, H. W.; Liu, Q.; Zhao, X. Z. In Situ Synthesis of NiS Nanowall Networks on Ni Foam as a TCO-Free Counter Electrode for Dye-Sensitized Solar Cells. *ACS Appl. Mater. Interfaces* **2014**, *6*, 5525−5530.
(25) Shi, J. J.; Luo, Y. H.; Wei, H. Y.; Luo, J. H.; Dong, J.; Lv, S. T.; Xiao, J. Y.; Xu, Y. Z.; Zhu, L. F.; Xu, X.; Wu, H. J.; Li, D. M.; Meng, Q. B. Modified Two-Step Deposition Method for High-Efficiency TiO_2/$CH_3NH_3PbI_3$ Heterojunction Solar Cells. *ACS Appl. Mater. Interfaces* **2014**, *6*, 9711−9718.
(26) Abrusci, A.; Stranks, S. D.; Docampo, P.; Yip, H. L.; Jen, A. K.; Snaith, H. J. High-Performance Perovskite−Polymer Hybrid Solar Cells via Electronic Coupling with Fullerene Monolayers. *Nano Lett.* **2013**, *13*, 3124−3128.
(27) Laban, W. A.; Etgar, L. Depleted Hole Conductor-Free Lead Halide Iodide Heterojunction Solar Cells. *Energy Environ. Sci.* **2013**, *6*, 3249−3253.
(28) Liu, M. Z.; Johnston, M. B.; Snaith, H. J. Efficient Planar Heterojunction Perovskite Solar Cells by Vapour Deposition. *Nature* **2013**, *501*, 395−398.
(29) Gregg, B. A.; Pichot, F.; Ferrere, S.; Fields, C. L. Interfacial Recombination Processes in Dye-Sensitized Solar Cells and Methods to Passivate the Interfaces. *J. Phys. Chem. B* **2001**, *105*, 1422−1429.
(30) Ito, S.; Liska, P.; Comte, P.; Charvet, R.; Pechy, P.; Bach, U.; Schmidt-Mende, L.; Zakeeruddin, S. M.; Kay, A.; Nazeeruddin, M. K.; Grätzel, M. Control of Dark Current in Photoelectrochemical (TiO_2/I^--I_3^-) and Dye-Sensitized Solar Cells. *Chem. Commun.* **2005**, *34*, 4351−4353.
(31) Shi, J. J.; Dong, J.; Lv, S. T.; Xu, Y. Z.; Zhu, L. F.; Xiao, J. Y.; Xu, X.; Wu, H. J.; Li, D. M.; Luo, Y. H.; Meng, Q. B. Hole-Conductor-Free Perovskite Organic Lead Iodide Heterojunction Thin-Film Solar Cells: High Efficiency and Junction Property. *Appl. Phys. Lett.* **2014**, *104*, 063901.
(32) Zhan, Z. Y.; An, J. N.; Zhang, H. C.; Hansen, R. V.; Zheng, L. X. Three-Dimensional Plasmonic Photoanodes Based on Au-Embedded TiO_2 Structures for Enhanced Visible-Light Water Splitting. *ACS Appl. Mater. Interfaces* **2014**, *6*, 1139−1144.
(33) Chang, H. M.; Yang, Y. J.; Li, H. C.; Hsu, C. C.; Cheng, I. C.; Chen, J. Z. Preparation of Nanoporous TiO_2 Films for DSSC Application by a Rapid Atmospheric Pressure Plasma Jet Sintering Process. *J. Power Sources* **2013**, *234*, 16−22.
(34) Kim, H.-S.; Mora-Sero, I.; Gonzalez-Pedro, V.; Fabregat-Santiago, F.; Juarez-Perez, E. J.; Park, N.-G.; Bisquert, J. Mechanism of Carrier Accumulation in Perovskite Thin-Absorber Solar Cells. *Nat. Commun.* **2013**, *4*, 2242.
(35) Gonzalez-Pedro, V.; Juarez-Perez, E. J.; Arsyad, W.-S.; Barea, E. M.; Fabregat-Santiago, F.; Mora-Sero, I.; Bisquert, J. General Working Principles of $CH_3NH_3PbX_3$ Perovskite Solar Cells. *Nano Lett.* **2014**, *14*, 888−893.
(36) Juarez-Perez, E. J.; Wußler, M.; Fabregat-Santiago, F.; Lakus-Wollny, K.; Mankel, E.; Mayer, T.; Jaegermann, W.; Mora-Sero, I. Role of the Selective Contacts in the Performance of Lead Halide Perovskite Solar Cells. *J. Phys. Chem. Lett.* **2014**, *5*, 680−685.
(37) Rong, Y. G.; Ku, Z. L.; Mei, A. Y.; Liu, T. F.; Xu, M.; Ko, S.; Li, X.; Han, H. W. Hole-Conductor-Free Mesoscopic TiO_2/$CH_3NH_3PbI_3$ Heterojunction Solar Cells based on Anatase Nanosheets and Carbon Counter Electrodes. *J. Phys. Chem. Lett.* **2014**, *5*, 2160−2164.